

Calibration and Validation for the SWIR-based Ocean Color Data Processing

Menghua Wang

Wei Shi and SeungHyun Son

NOAA/NESDIS/STAR
E/RA3, Room 102, 5200 Auth Road
Camp Springs, MD 20746, USA

Menghua.Wang@noaa.gov

*AERONET-OC International Workshop
JPSS Program Office, Greenbelt, Maryland, February 23-24, 2010*

Acknowledgements

JPSS/IOP ocean Cal/Val support, NOAA/NASA funding, NASA SeaBASS in situ data, **MOBY** data, in situ data from Lake Taihu (J. Tang), and MODIS Level 1B data.



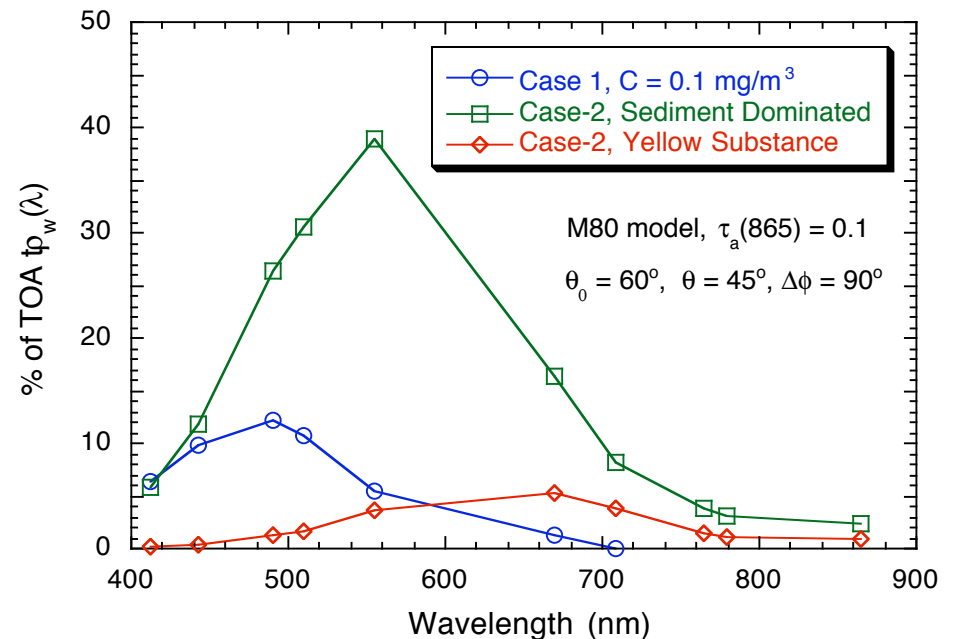
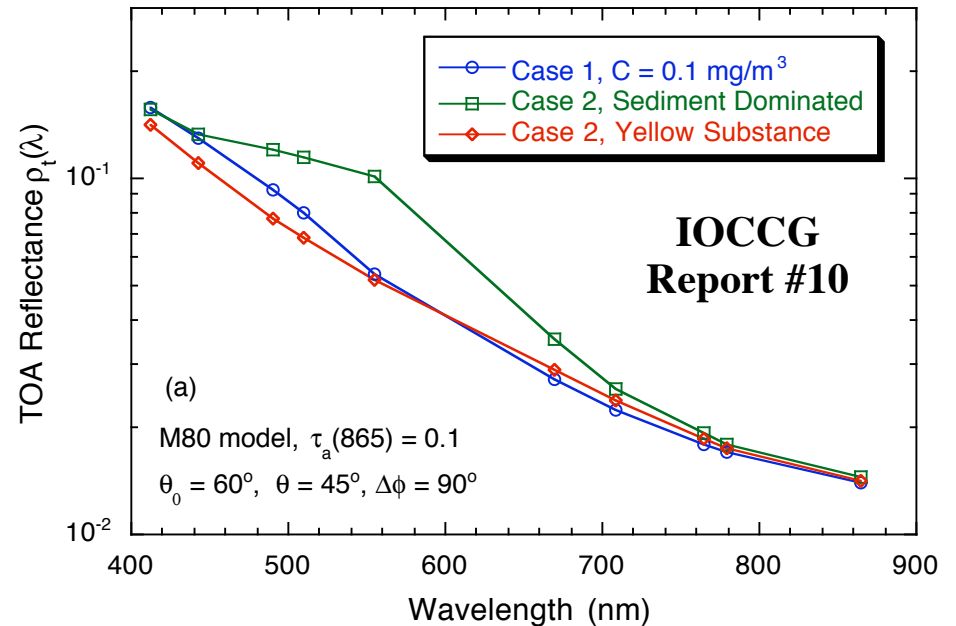
Background

➤ At satellite altitude ~90% sensor-measured signal over ocean comes from the atmosphere & surface

- Require accurate **atmospheric correction** and **calibration**.
- **0.5%** error in the TOA radiance corresponds to possible of **~5%** in the derived ocean water-leaving radiance.
- We need **~0.1%** sensor calibration accuracy.

➤ Atmospheric correction algorithm

- Using the near-infrared (**NIR**) bands, e.g., Gordon & Wang (1994) for SeaWiFS/MODIS (open oceans)
- Using the shortwave infrared (**SWIR**) bands, e.g., MODIS 1240 and 2130 nm bands (turbid waters)
- **NIR-SWIR** combined algorithm (Wang & Shi, 2007) for open oceans and costal turbid waters.



Vicarious Calibration (VC)

For ocean color remote sensing, post-launch vicarious calibration is necessary for visible bands.

VC: Calibration of whole system: Sensor + Algorithms

- Account for (by direct measurement or prediction) all of the components of the TOA radiance and
- Compare the results with the sensor-measured radiance.

Sensor-measured reflectance:

$$\rho_t^{(Meas)}(\lambda) = [1 + a(\lambda)]\rho_t(\lambda), \quad a(\lambda) - \text{calibration error}$$

Computed reflectance:

$$\rho_t^{(Computed)}(\lambda) = \underbrace{\rho_r(\lambda)}_{\text{Computed}} + \underbrace{\rho_a(\lambda) + \rho_{ra}(\lambda)}_{\text{Predicted Using Models}} + \underbrace{t\rho_{wc}(\lambda)}_{\text{Computed}} + \underbrace{t\rho_w(\lambda)}_{\text{Measured}}$$

H. R. Gordon, "In-orbit calibration strategy for ocean color sensors," *Remote Sens. Environ.*, **63**, 265-278, 1998.

Calibration Site, e.g., MOBY

Vicarious Calibration (Cont.)

Corrected reflectance after vicarious calibration (VC):

$$\rho_t^{(Corrected)}(\lambda) = G^{(VC)}(\lambda)\rho_t^{(Meas)}(\lambda) = [1 + a'(\lambda)]\rho_t(\lambda)$$

where for a given calibration site (solar and viewing geometry)

$$a'(\lambda) = G^{(VC)}(\lambda)[1 + a(\lambda)] - 1 = \left[\rho_t^{(Computed)}(\lambda) \right]^{(VC)} / \rho_t(\lambda) - 1$$

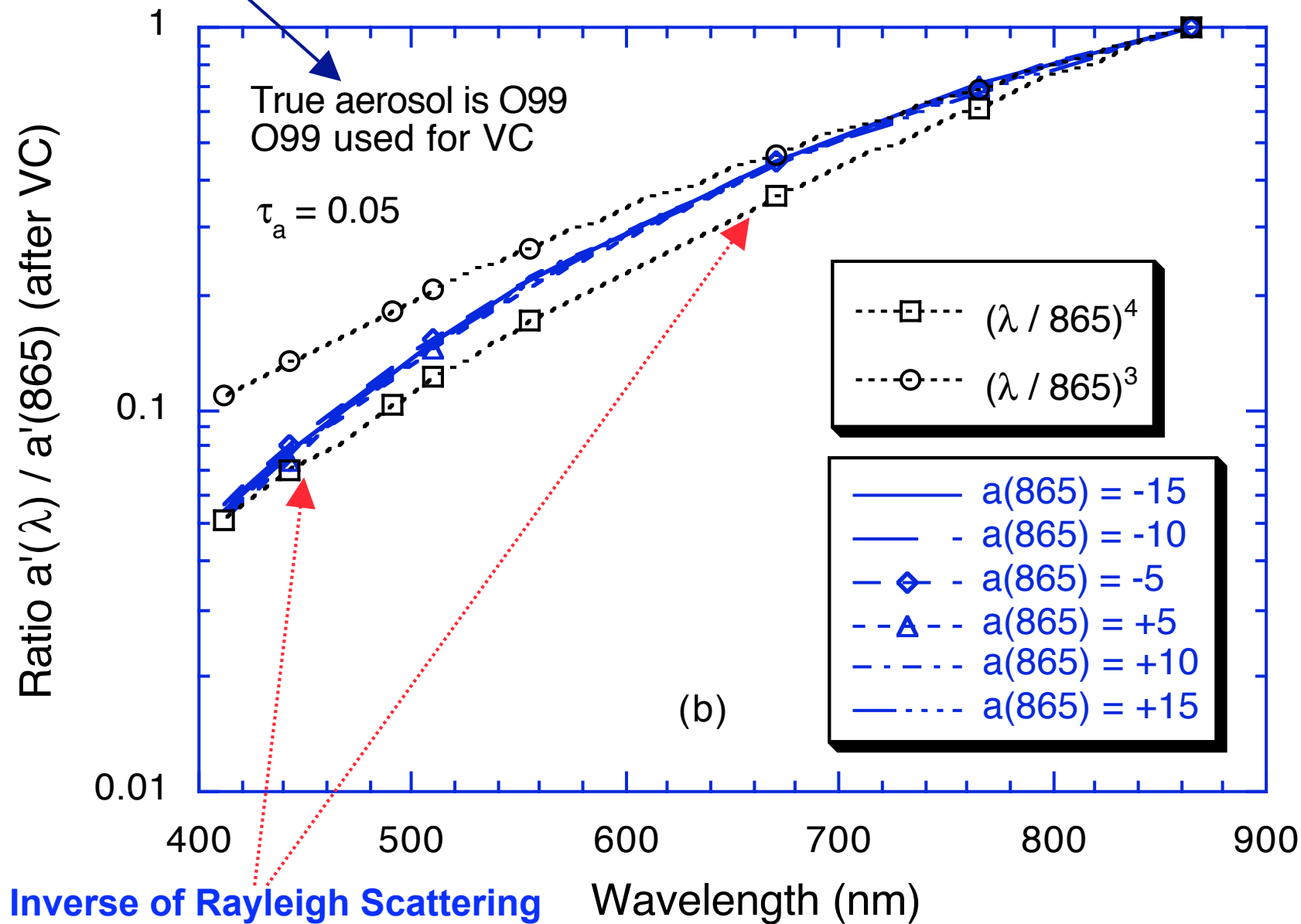
For $a'(\lambda)$ with $\lambda < 865 \text{ nm}$ only dependent on $a(865)$ (or at the SWIR band), but **not** on $a(\lambda)$.

Results of VC are independent of the sensor pre-launch calibration for $\lambda < 865 \text{ nm}$ (or SWIR 1240 nm)!!

Wang, M. and H. R. Gordon, "Calibration of ocean color scanners: How much error is acceptable in the near-infrared," *Remote Sens. Environ.*, **82**, 497-504, 2002.

Used correct aerosol model

$$a'(865) = a(865)$$

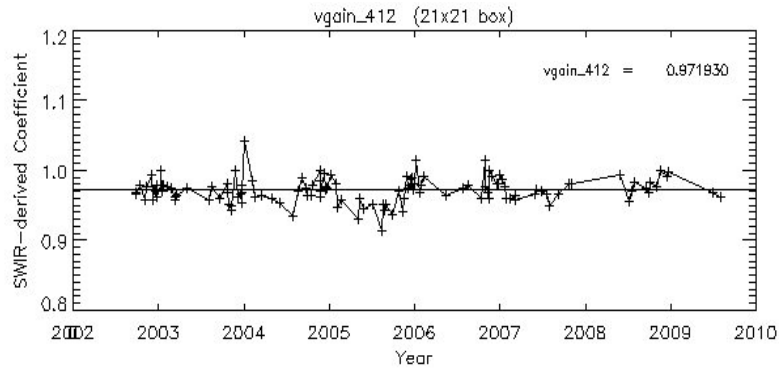


Examples of VC for SWIR and NIR-based Algorithms Using $nL_w(\lambda)$ Spectra Sources:

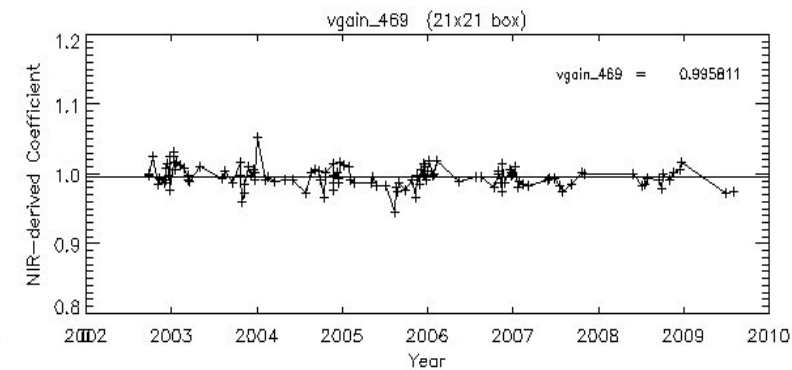
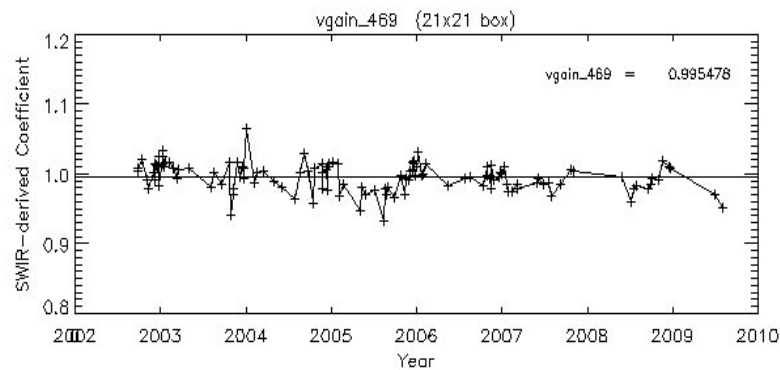
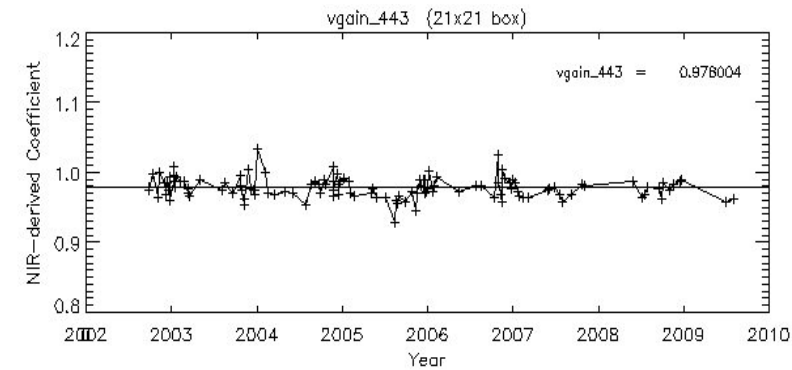
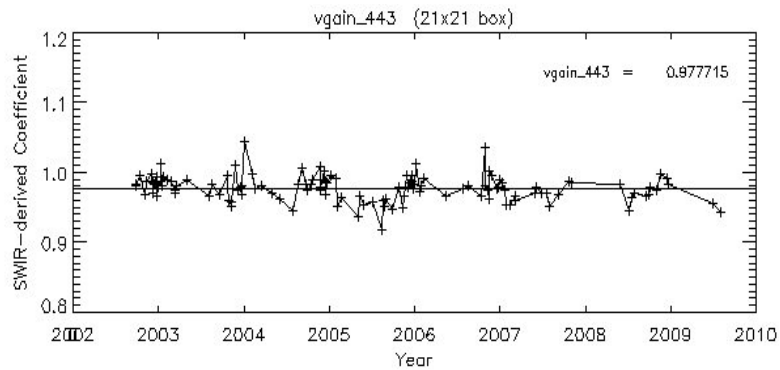
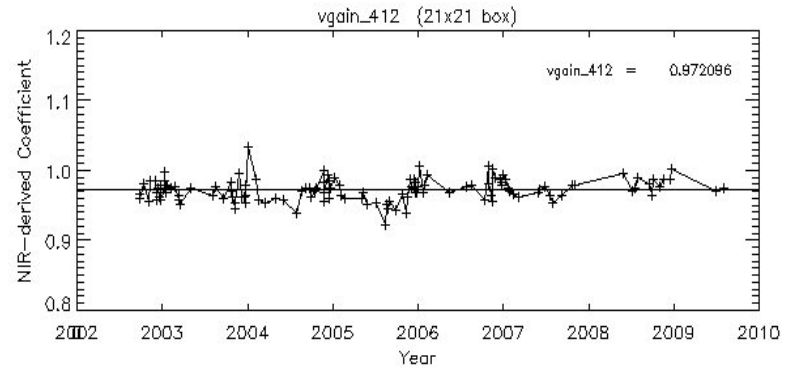
- From MODIS-Aqua Standard Products in Hawaii Calibration Site (Satellite-to-Satellite, Wang, 2006)
- From MOBY In Situ Data in Hawaii Calibration Site

SWIR vs. NIR-Based VC Gains from **MOBY** In Situ $nL_w(\lambda)$

SWIR-based



NIR-based



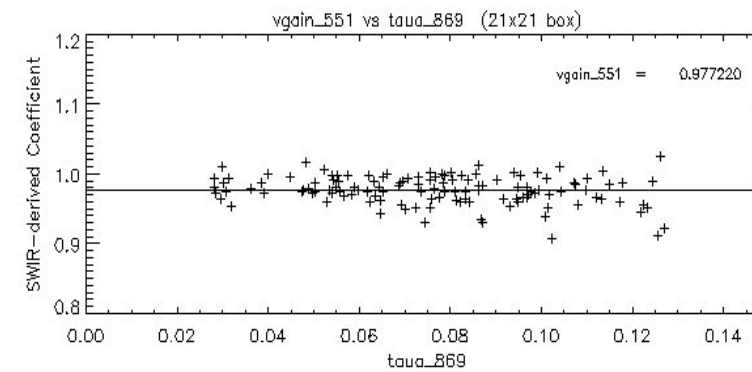
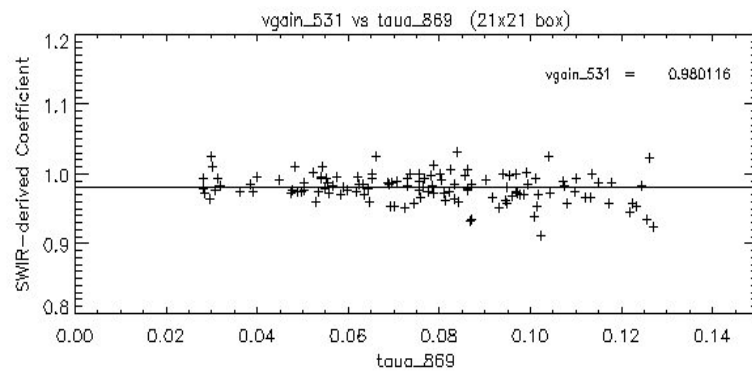
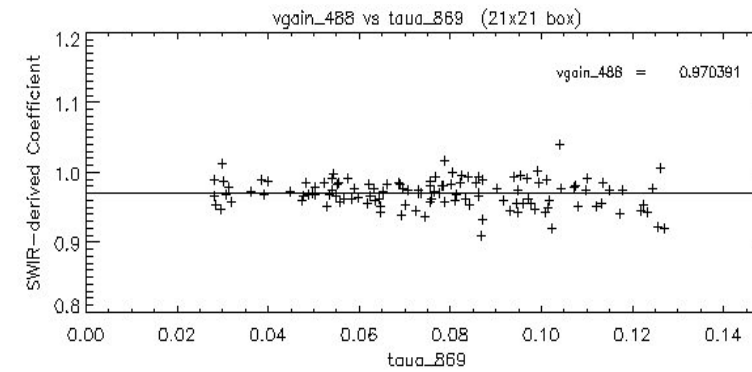
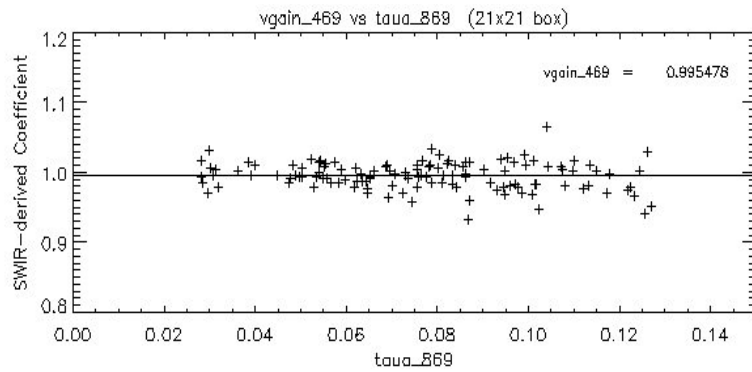
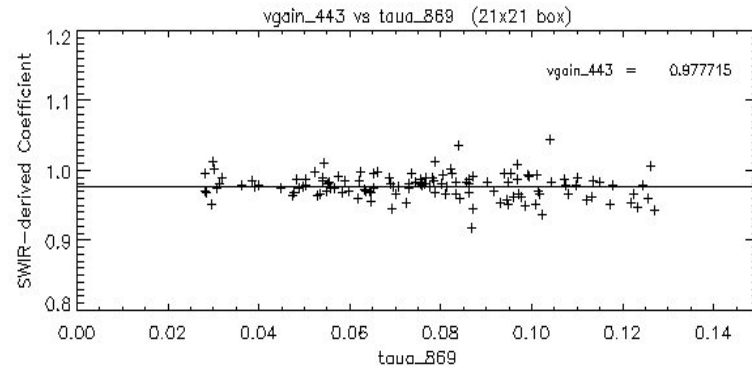
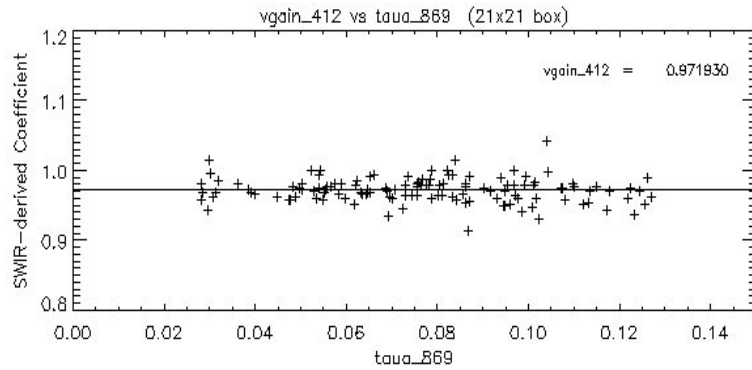
Vicarious Gains Derived from **Four** Different Ways

SWIR and NIR VC Gains				
Wavelength (nm)	$nL_w(\lambda)$ Source from MODIS-Aqua		$nL_w(\lambda)$ Source from MOBY In Situ	
	SWIR- derived Gains	NIR-derived Gains	SWIR- derived Gains	NIR-derived Gains
412	0.9747	0.9745	0.9719	0.9721
443	0.9768	0.9766	0.9777	0.9780
469	0.9811	0.9809	0.9955	0.9958
488	0.9697	0.9695	0.9704	0.9708
531	0.9820	0.9817	0.9801	0.9807
551	0.9730	0.9728	0.9772	0.9779
555	0.9786	0.9783	0.9798	0.9805
645	1.0089	1.0086	0.9877	0.9885
667	0.9767	0.9765	0.9795	0.9803
678	0.9699	0.9696	0.9727	0.9735
748	0.9722	–	0.9752	–
859	0.9869	–	0.9890	–
869	0.9836	–	0.9856	–

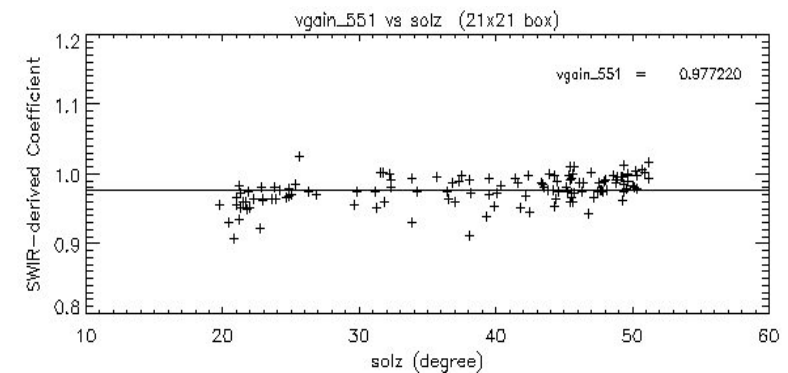
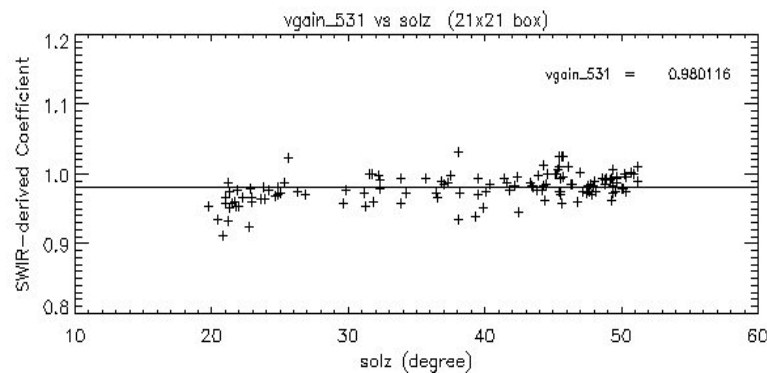
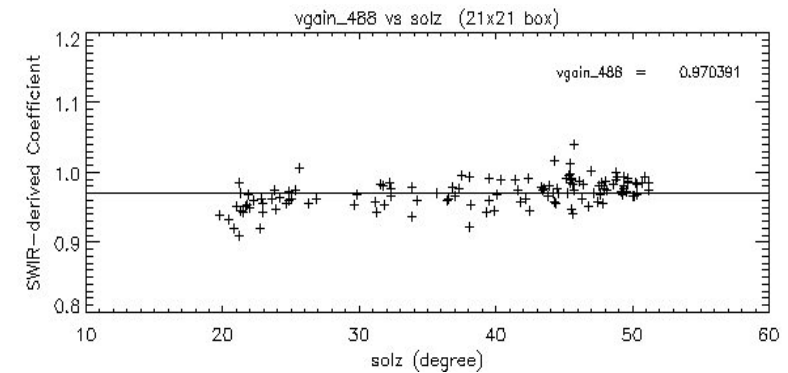
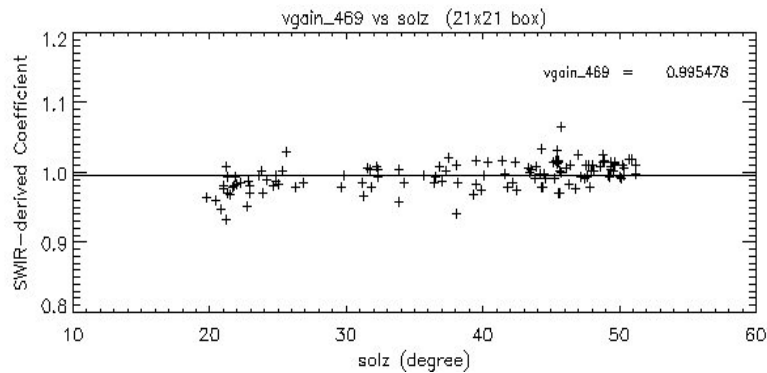
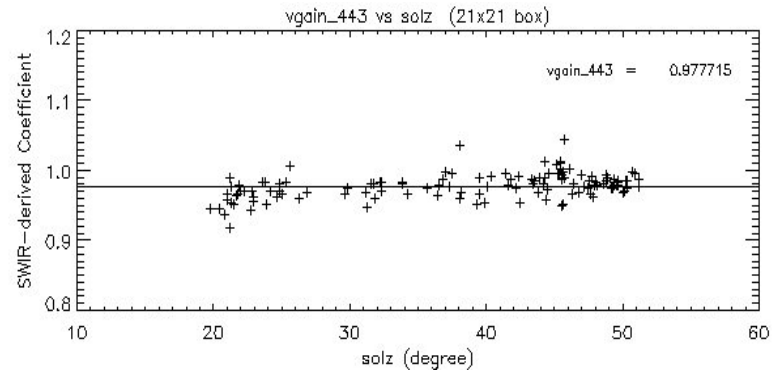
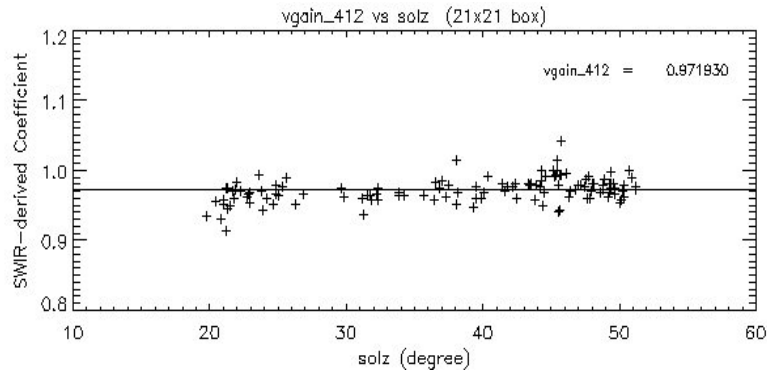
**Diff:
0.014**



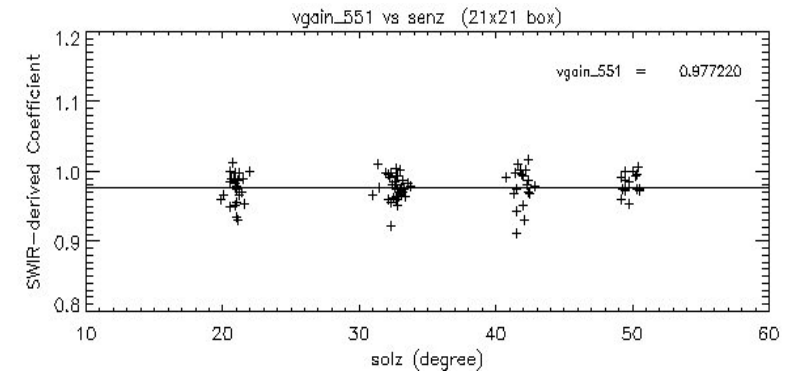
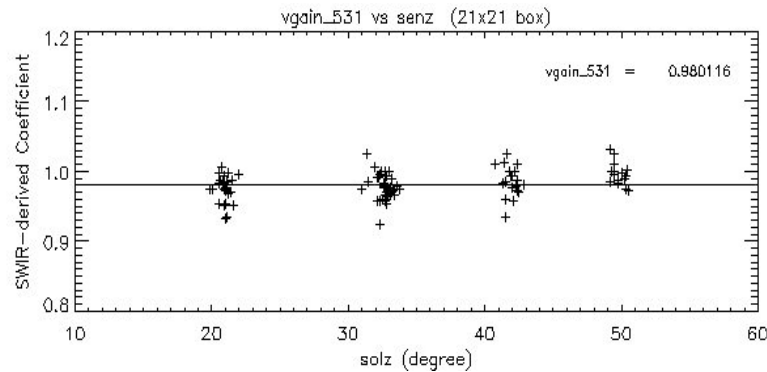
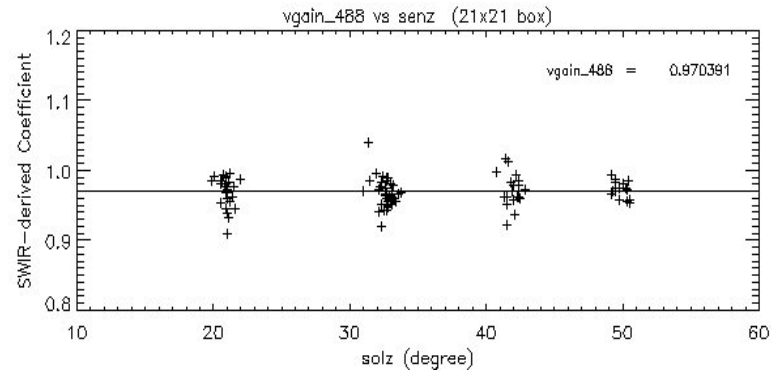
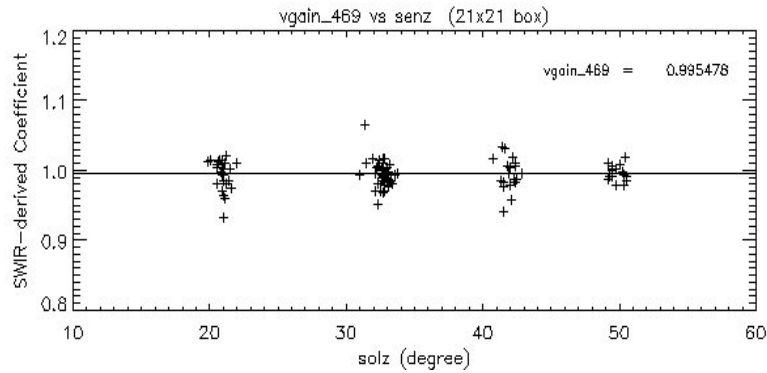
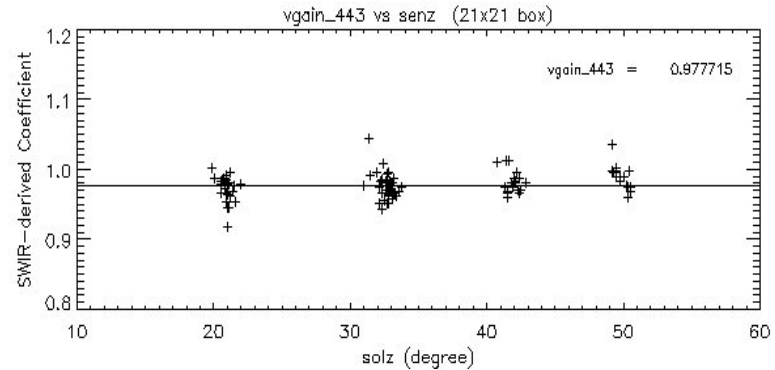
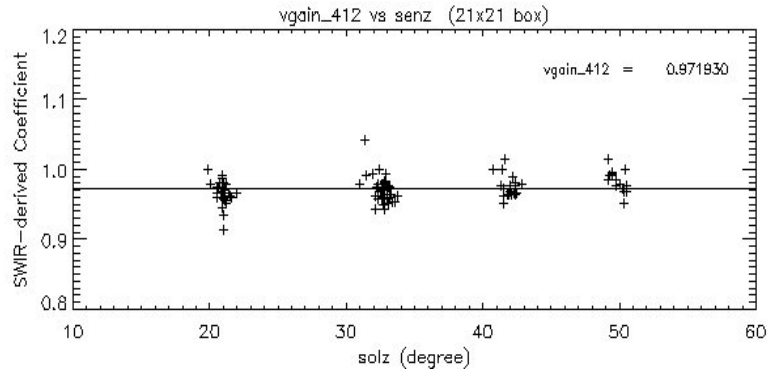
VC Gains vs. AOT (taua(869)) (Sensitivity Study-1)



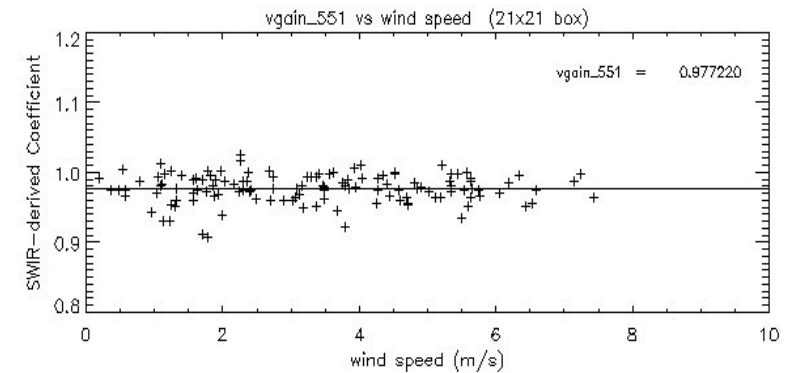
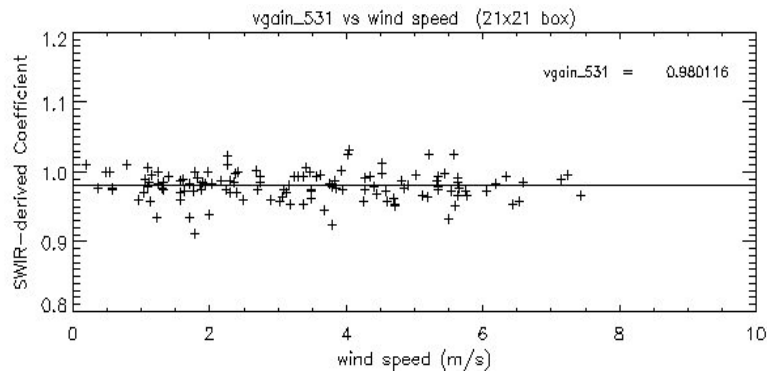
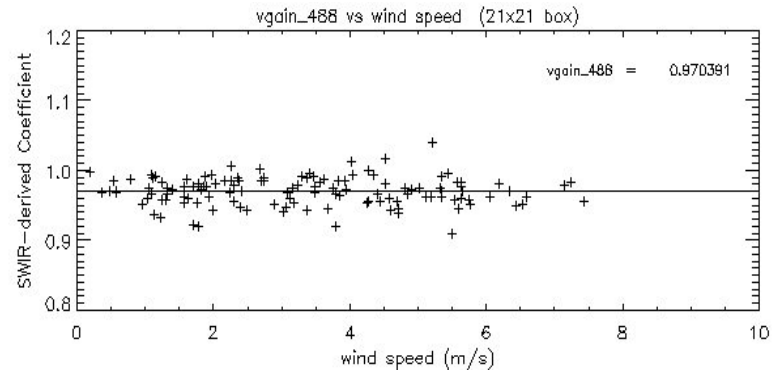
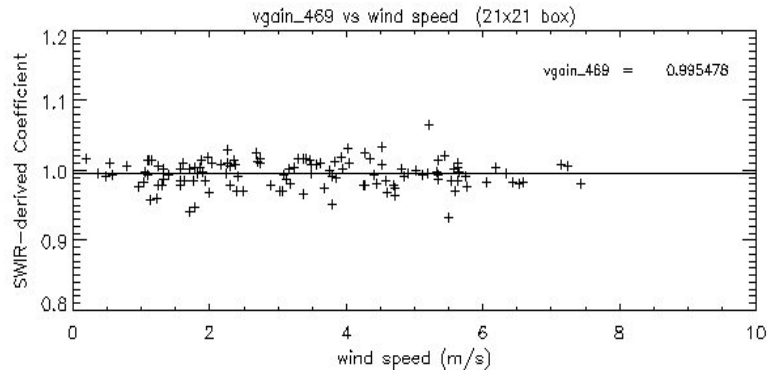
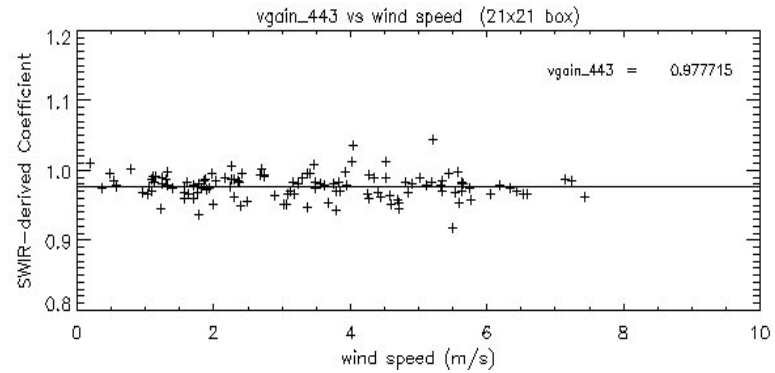
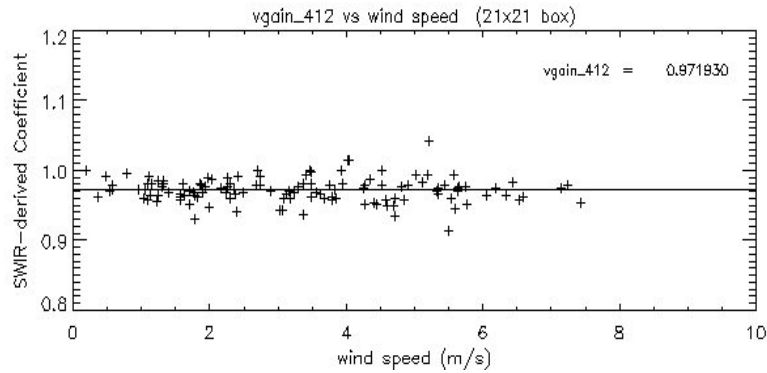
VC Gains vs. Solar-Zenith Angle (Sensitivity Study-2)



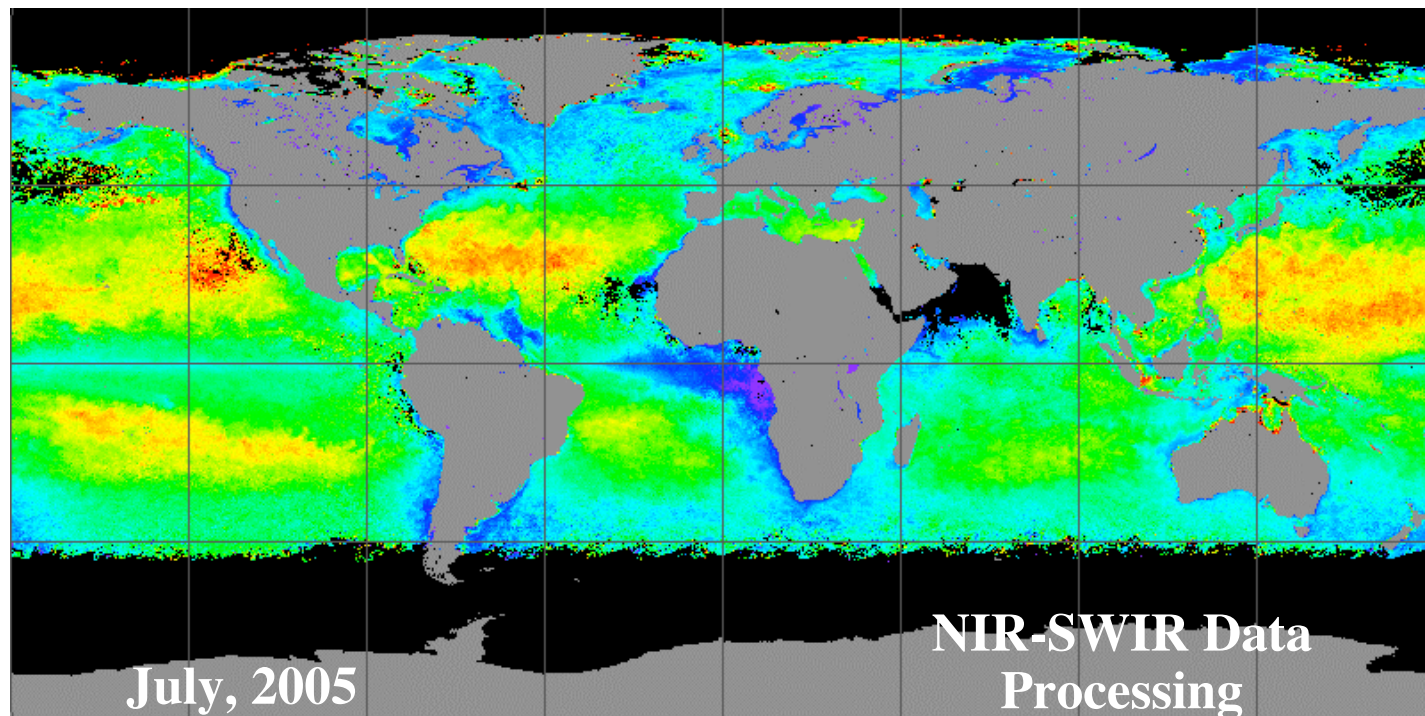
VC Gains vs. Sensor-Zenith Angle (Sensitivity Study-3)



VC Gains vs. Wind Speed (Sensitivity Study-4)



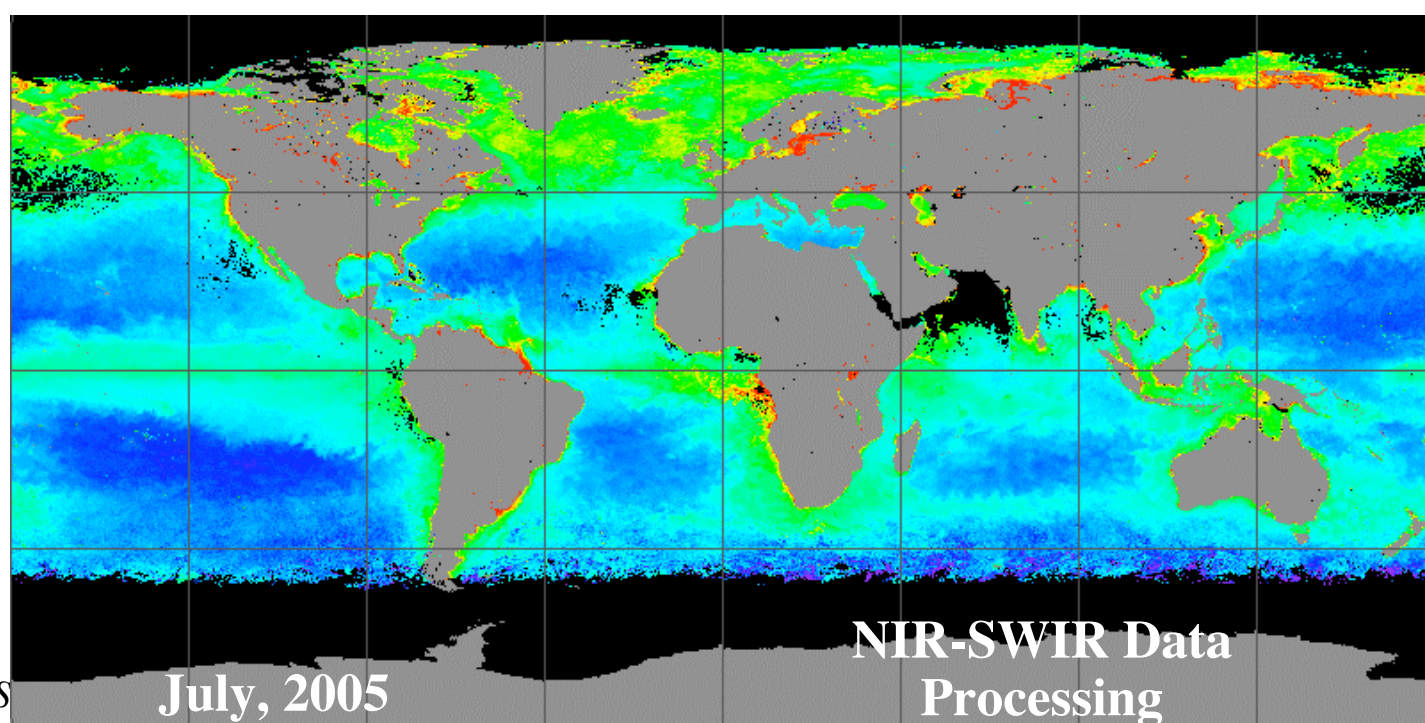
$nL_w(443)$
Scale: 0.-3.0
(mW/cm² μm sr)



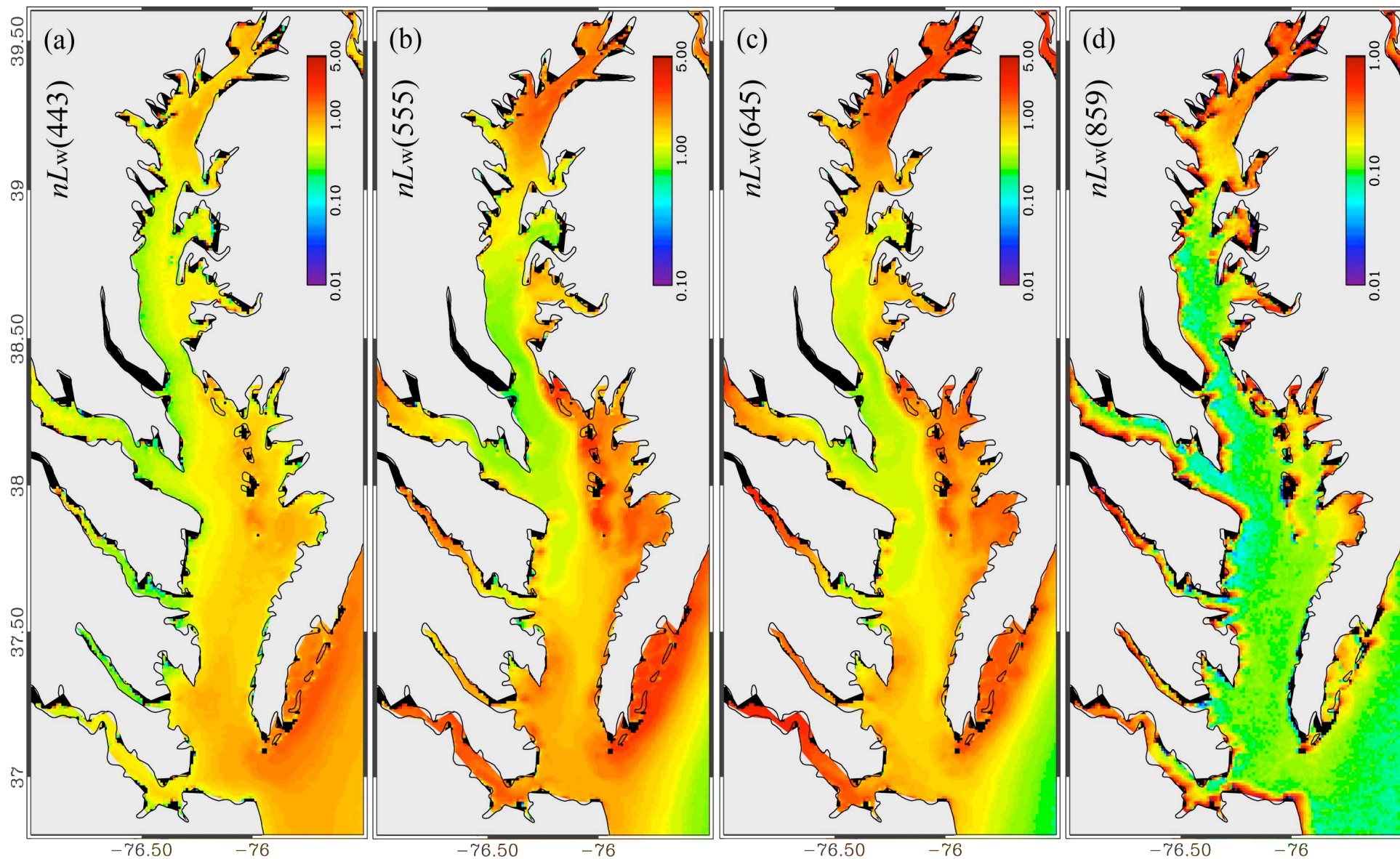
Chlorophyll-a
0.01-10 (mg/m³)
(Log scale)

Wang, M., S. Son, and W. Shi
(2009), "Evaluation of
MODIS SWIR and NIR-
SWIR atmospheric
correction algorithms
using SeaBASS data,"
Remote Sens. Environ.,
113, 635-644.

Menghua Wang, NOAA/NES

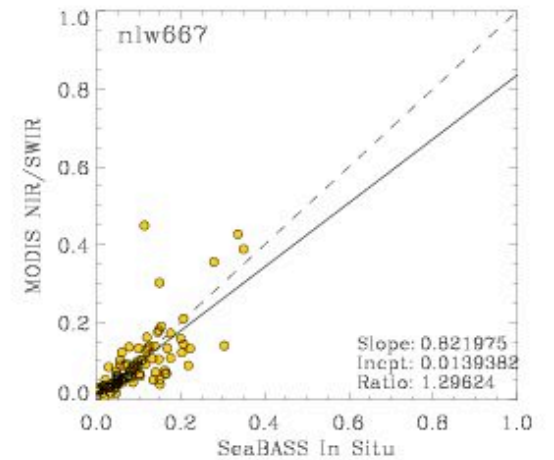
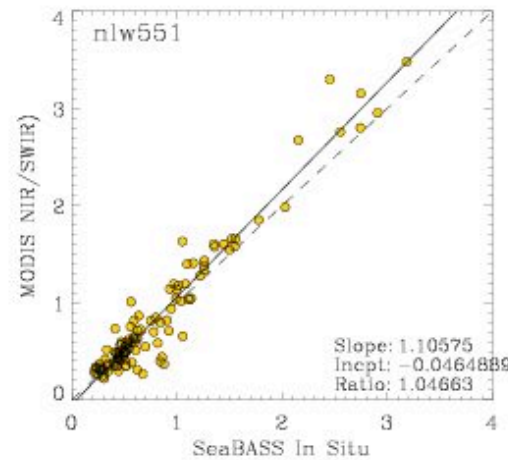
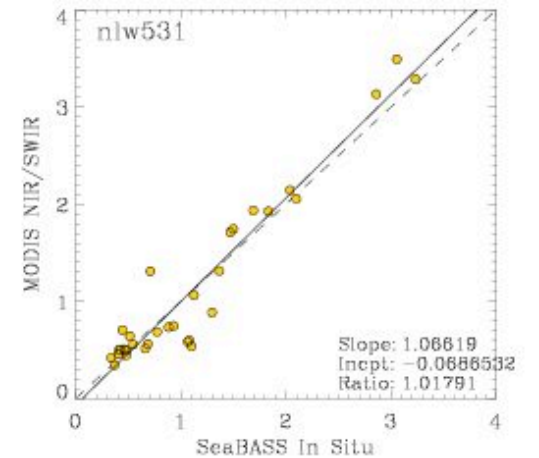
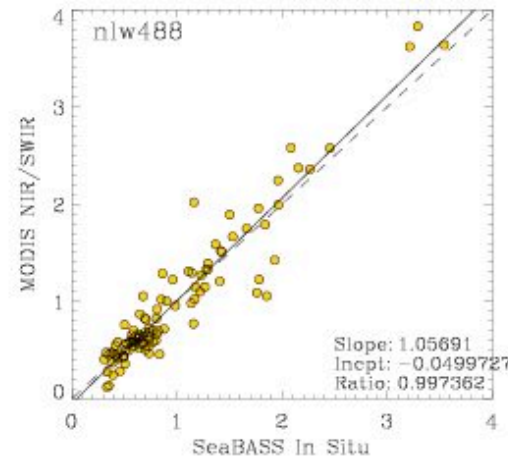
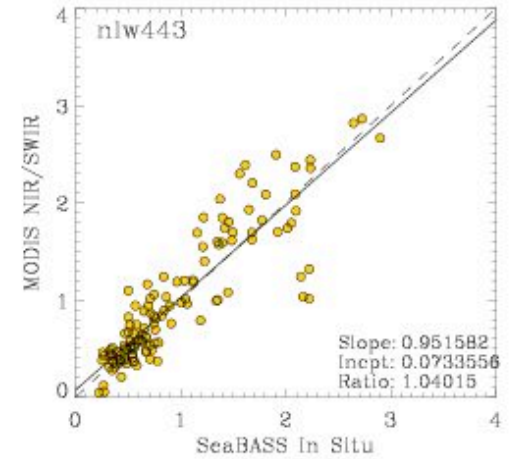
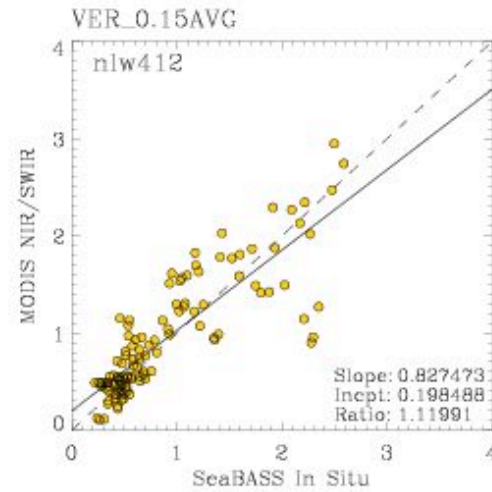
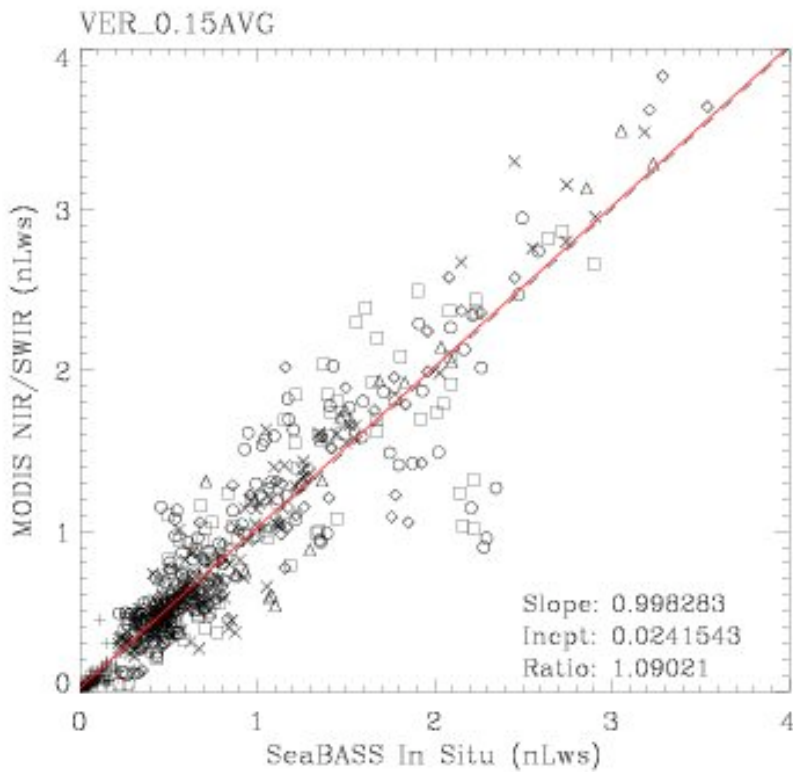


Climatology (Jul 2002-Dec 2010) Images of MODIS NIR-SWIR nL_w

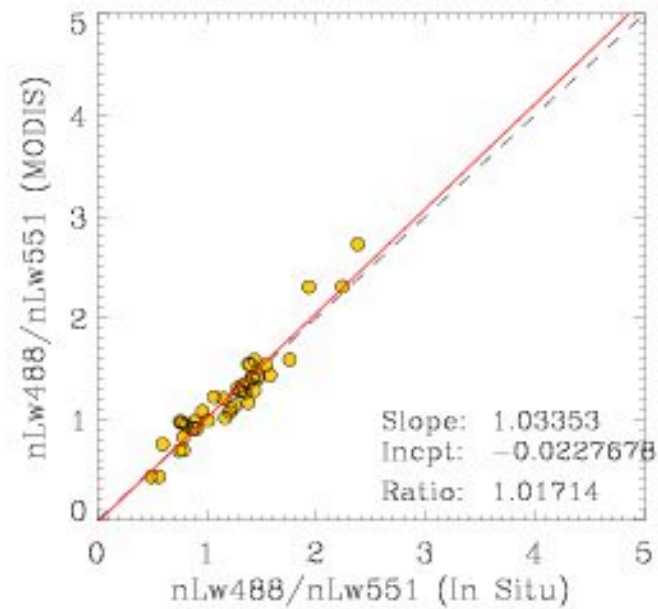
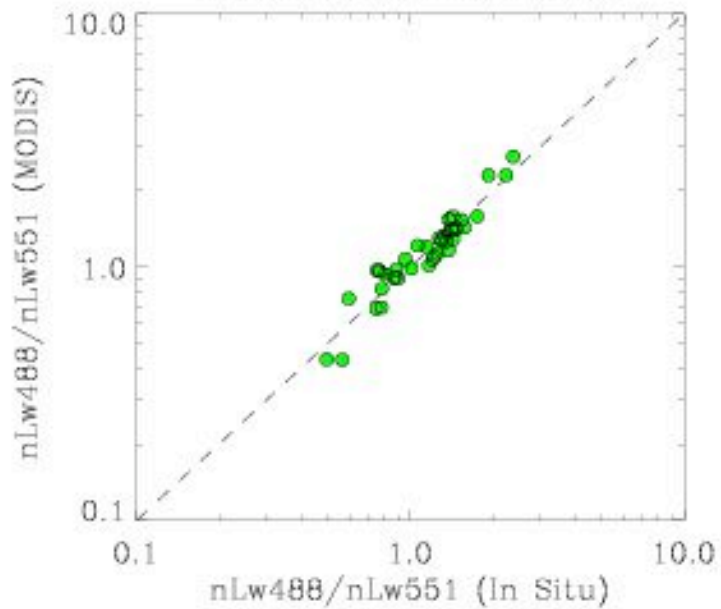
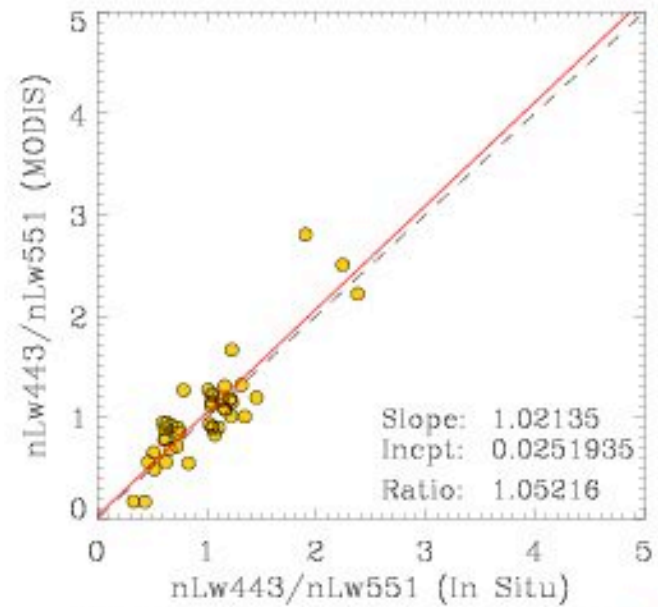
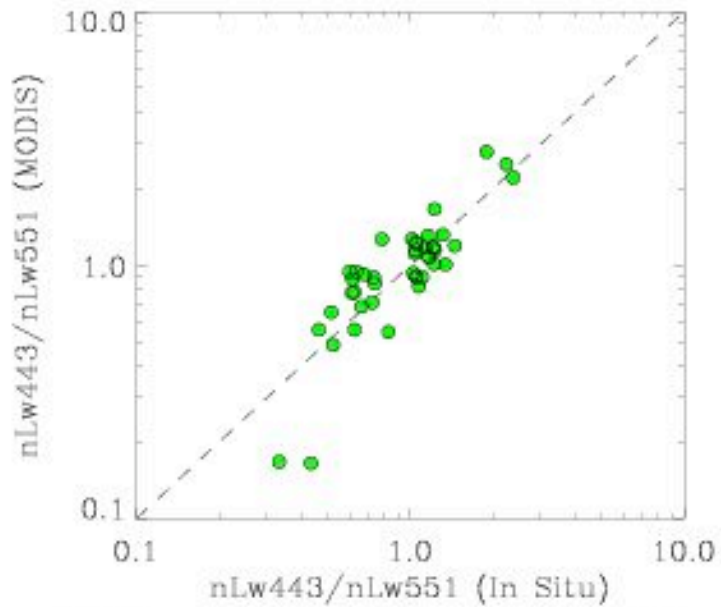


- MODIS-Aqua ocean color products were derived and compared with the SeaBASS in situ data.
- **Example results** are provided with the VC gains derived from **MOBY** data using the **SWIR** approach (presented in the previous Table).

Matchup Comparisons with In Situ Data



Radiance Band Ratio Results (MODIS vs. In Situ)



Comparisons Between MODIS and **In Situ** (SeaBASS) Data

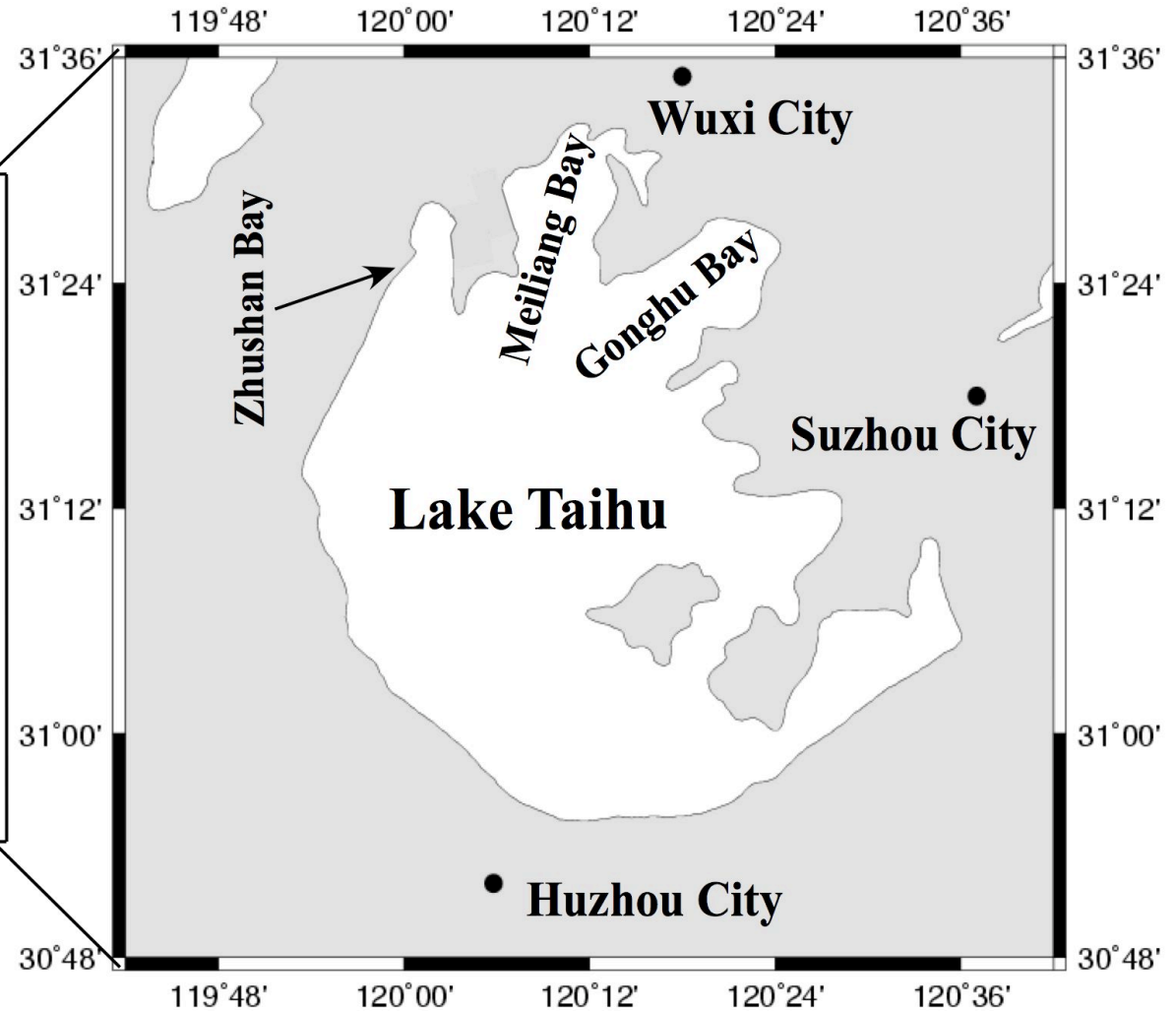
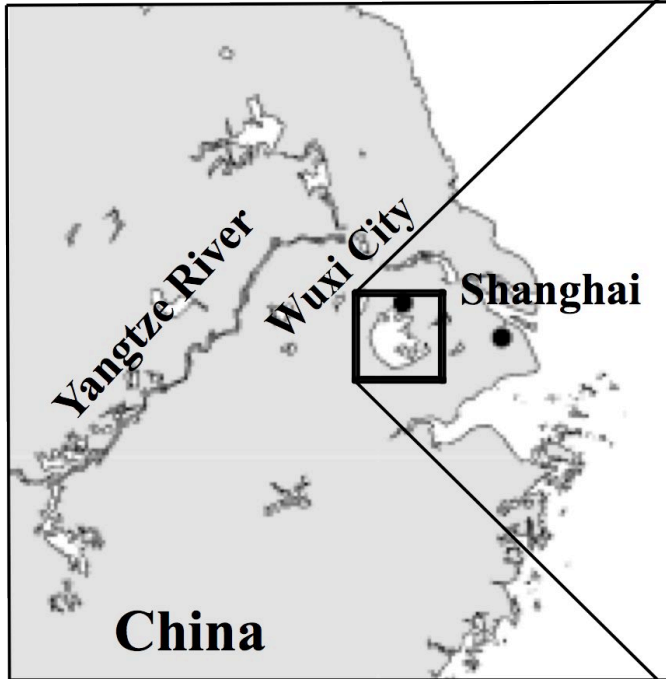
Product	Data #	NIR-SWIR Method				
		Slope	Int [†]	R [‡]	Mean Ratio [*]	Medium Ratio ^{&}
$nL_w(412)$	116	0.827	0.198	0.873	1.120	1.084
$nL_w(443)$	128	0.952	0.073	0.891	1.040	1.025
$nL_w(488)$	104	1.057	-0.050	0.951	0.997	1.015
$nL_w(531)$	32	1.066	-0.069	0.961	1.018	1.040
$nL_w(551)$	116	1.106	-0.046	0.968	1.047	1.055
$nL_w(667)$	97	0.822	0.014	0.727	1.296	1.129
Overall $nL_w(\lambda)$	593	0.998	0.024	0.935	1.090	1.030
$nL_w(443)/$ $nL_w(551)$	43	1.021	0.025	0.879	1.052	1.032
$nL_w(488)/$ $nL_w(551)$	43	1.034	-0.023	0.953	1.017	0.996

[†]Intercept for line fit [‡]Correlation coefficient

^{*}Mean ratio of MODIS vs. in situ data [&]Medium ratio of MODIS vs. in situ data

Geo-location of Lake Taihu

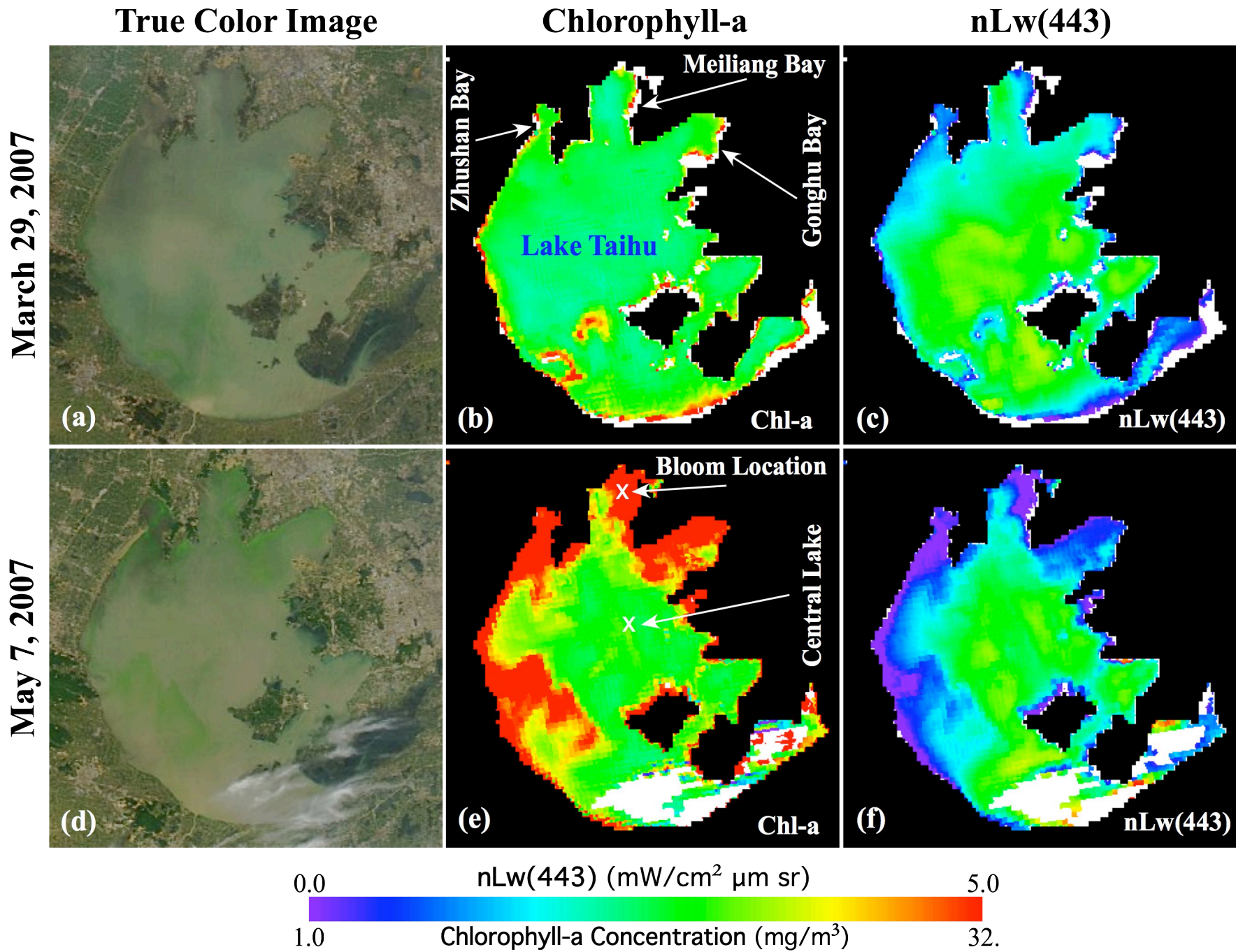
**Extremely
Turbid Waters**



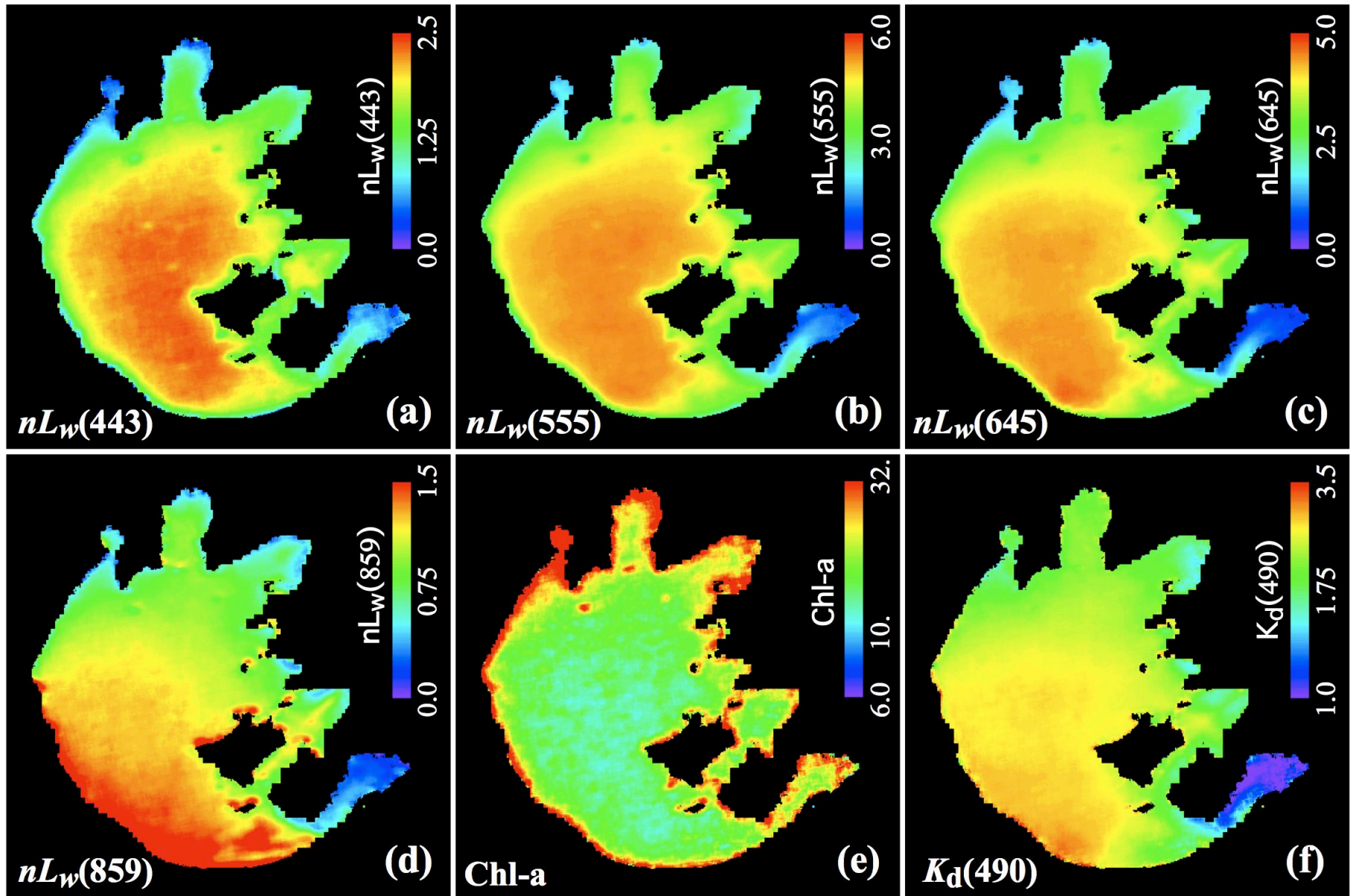
- ✓ The third largest fresh inland lake in China (~2,250 km²).
- ✓ Located in one of the world's most urbanized and heavily populated areas.
- ✓ Provide water resource for several million residents in nearby Wuxi city.

Methodology

- The SWIR atmospheric correction algorithm (Wang, 2007; Wang & Shi, 2005) is used for the water property data processing.
- Since MODIS 1240 nm band is not always black for the entire Lake Taihu, we have developed three-step method in the data processing for each MODIS-Aqua data file:
 - ✓ First, regions for the black of 1240 nm band are determined using the SWIR data processing.
 - ✓ Second, a dominant aerosol model from the region with black of 1240 nm band is obtained, and
 - ✓ Finally, with the derived aerosol model, the SWIR atmospheric correction algorithm is run using only 2130 nm band (with fixed aerosol model).
- The Lake Taihu water property data are then derived.



MODIS-Measured Climatology Water Color Property for Lake Taihu



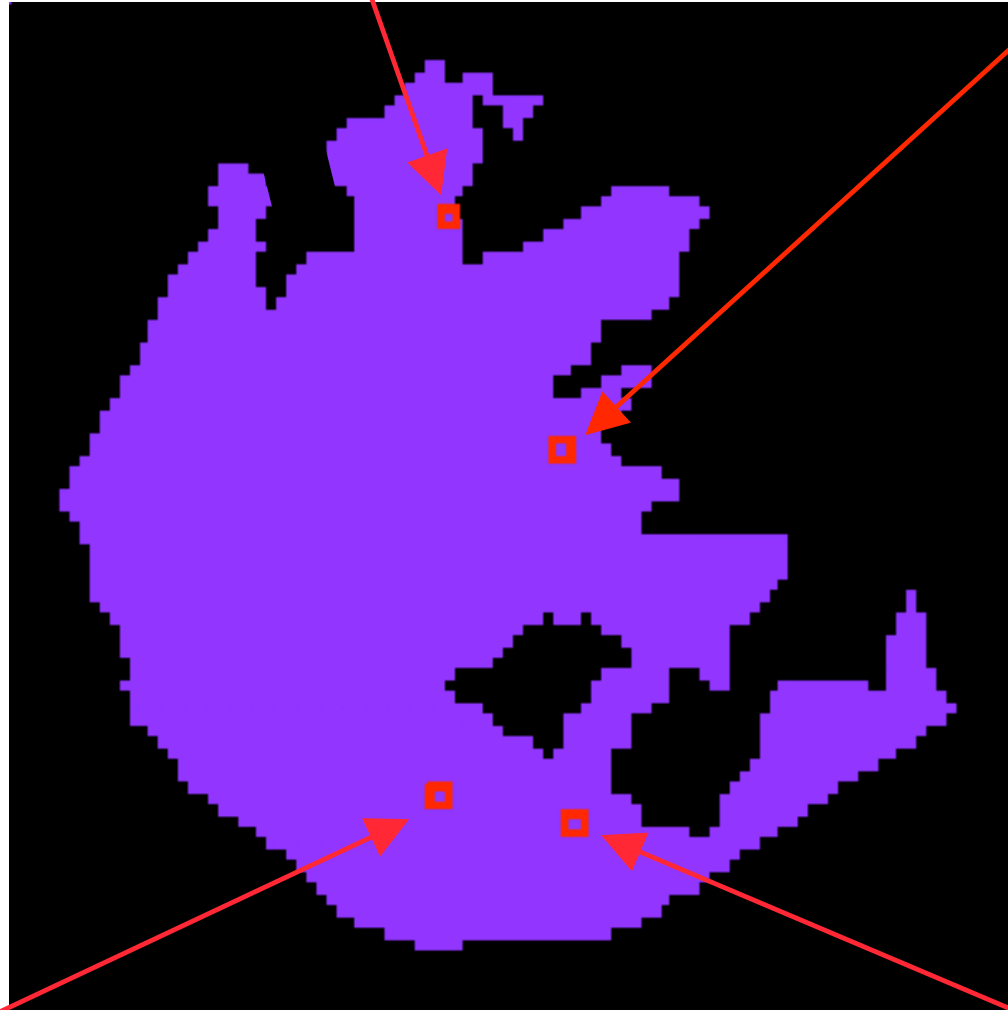
Wang, M., W. Shi, J. Tang (2011), "Water property monitoring and assessment for China's inland Lake Taihu from MODIS-Aqua measurement," *Remote Sens. Environ.*, **115**, 841-854.

Menghua Wang, NOAA/NESDIS/STAR

In Situ Data

(a) June 10, 2007

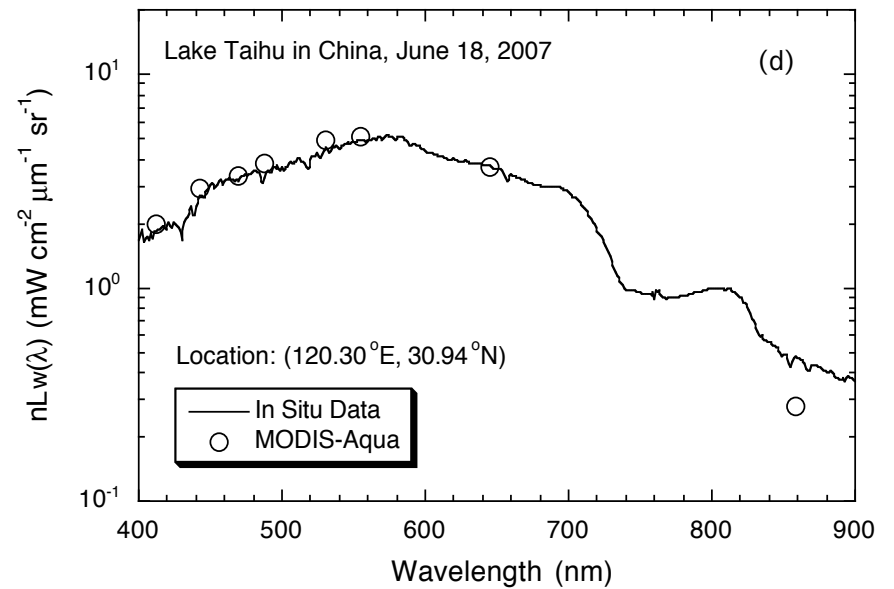
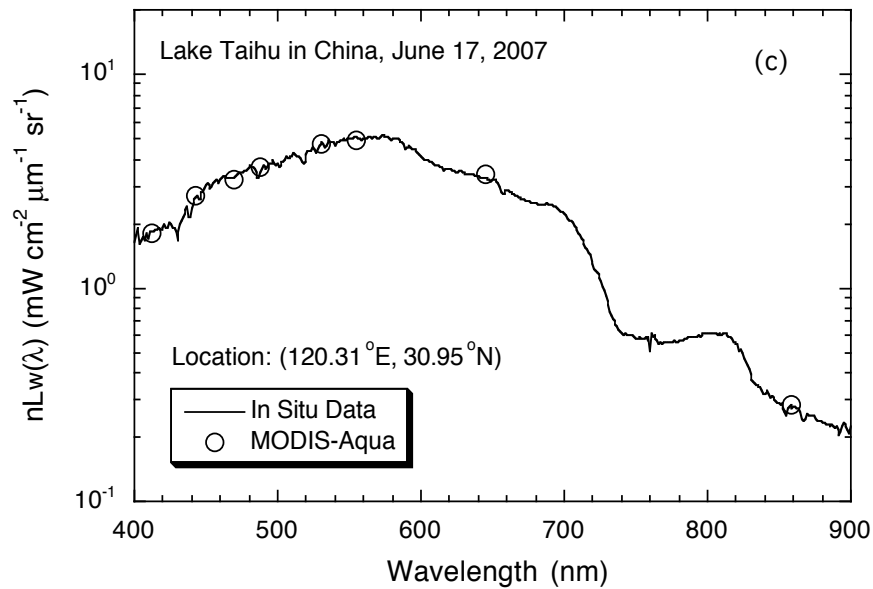
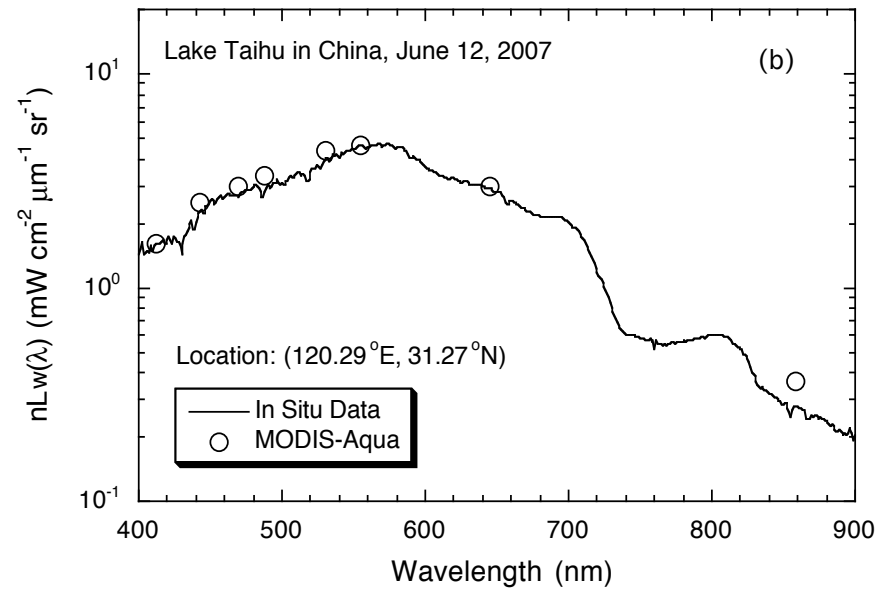
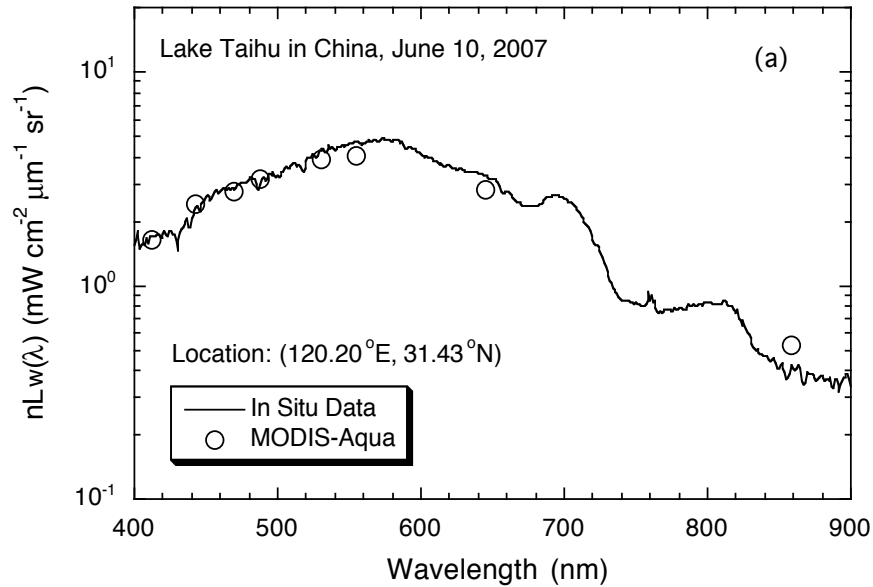
(b) June 10, 2007



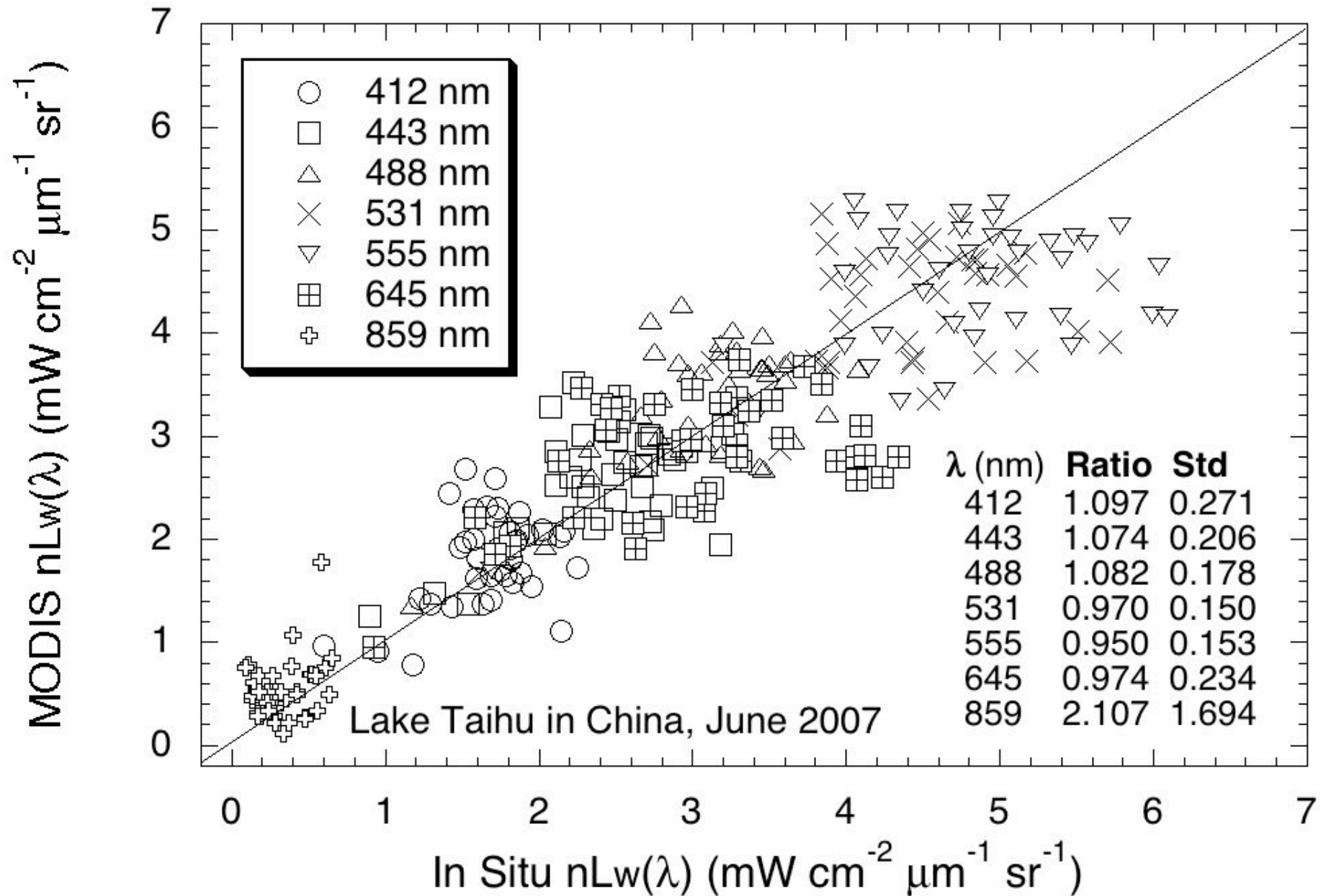
(d) June 18, 2007

(c) June 17, 2007

Validation Results for MODIS-derived Water-leaving Radiance Spectra



Validation Results in Lake Taihu



Thank You!